Consistency of Three Kalman Filter Extensions in Hybrid Navigation

Simo Ali-Löytty, Niilo Sirola & Robert Piché
Institute of Mathematics
Tampere University of Technology

simo.ali-loytty@tut.fi

Abstract

A filter is *consistent* if predicted errors are at least as large as actual errors. In this paper, we evaluate the consistency of three filters and illustrate what could happen if filters are inconsistent. Our application is hybrid positioning which is based on signals from satellites and from mobile phone network base stations. Examples show that the consistency of a filter is very important. We evaluate three filters: EKF, EKF2 and PKF. Extended Kalman Filter (EKF) solves the filtering problem by linearizing functions. EKF is very commonly used in satellite-based positioning and it has also been applied in hybrid positioning. We show that nonlinearities are insignificant in satellite measurements but often significant in base station measurements. Because of this, we also apply Second Order Extended Kalman Filter (EKF2) in hybrid positioning. EKF2 is an elaboration of EKF that takes into consideration the nonlinearity of the measurement models. The third filter is called Position Kalman Filter (PKF), which filters a sequence of static positions and velocities. We also check what kind of measurement combinations satisfy CGALIES and FCC requirements for location.

1 Introduction

In navigation, filters are used to compute an estimate of the position using current and past measurement data. When the number of measurements is insufficient to specify a unique position solution, the filtered estimate may veer away from the true route and get stuck in an incorrect solution branch. For filters to avoid and recover from such mistakes, it is important that they are *consistent*, that is, their predicted errors should be at least as large as actual errors. In Section 3.5, we define a filter consistency and introduce a test for filter inconsistency. In this study, we evaluate the consistency of three filters which are representative of the Kalman type filters used in hybrid navigation based on signals from satellites and from mobile phone network base stations. The reason why we concentrate on Kalman type filters is that they are fast to compute. It is possible, for example with particle filters and grid-based methods, to get a more accurate estimate, but such filters are slower and because of this they do not yet suit mobile positioning.

2 Problem statement

2.1 Target

In this section, we introduce our problem. First of all, we model the user state $\mathbf{x}$ and measurements $\mathbf{y}$ as stochastic processes. We have an initial state $\mathbf{x}_0$ and a dynamic system

$$\begin{aligned} \mathbf{x}_k &= \mathbf{f}_{k-1}(\mathbf{x}_{k-1}) + \mathbf{w}_{k-1} \\ \mathbf{y}_k &= \mathbf{h}_k(\mathbf{x}_k) + \mathbf{v}_k, \end{aligned} \tag{1}$$

where subscript k represents time moment t_k, $k = 1, 2, \ldots$. We assume that all errors ($\mathbf{w}_k$ and $\mathbf{v}_k$) are zero mean, white and independent. The aim is to solve state conditional probability density function (cpdf)

$$f(\mathbf{x}_k | \mathbf{y}_{1:k} = y_{1:k}) \stackrel{\triangle}{=} f_{cpdf}(\mathbf{x}_k), \tag{2}$$

when conditional $\mathbf{y}_{1:k} \stackrel{\triangle}{=} \{\mathbf{y}_1, \ldots, \mathbf{y}_k\}$ are past and current measurements. These densities are usually called posterior densities and densities $f(\mathbf{x}_{k+1} | \mathbf{y}_{1:k} = y_{1:k})$ are called prior densities. Knowledge of the posterior density enables one to compute an optimal state estimate with respect to any criterion. For example, the minimum mean-square error (MMSE) estimate is the conditional mean of $\mathbf{x}_k$ [1, 15]. In general and in our case the conditional probability density function cannot be determined analytically.

In our applications, the state $\mathbf{x} = \left[\mathbf{r}_u^T, \mathbf{v}_u^T\right]^T$ consists of user position vector $\mathbf{r}_u$ and user velocity vector $\mathbf{v}_u$. State dynamics are specified in (6). Measurements $\mathbf{y}$ (19) consist of satellite pseudorange $\boldsymbol{\rho}^{\mathrm{s}}$ (11) and delta pseudorange $\dot{\boldsymbol{\rho}}^{\mathrm{s}}$ (12) measurements, and base station range measurements $\boldsymbol{\rho}^{\mathrm{b}}$ (18). We do not model user clock because it is quite difficult to get a realistic clock model. Therefore, we must use the difference measurements of satellites.

2.2 State dynamics

We use the position-velocity (PV) model, where the user velocity is a random walk process [2]. The user state is the solution of a stochastic differential equation

$$\mathbf{d}\mathbf{x}(t) = \mathrm{F}(t)\mathbf{x}(t)dt + \mathrm{G}(t)\mathbf{d}\boldsymbol{\beta}(t), \tag{3}$$

where

$$\mathrm{F}(t) = \begin{bmatrix} 0_{3\times3} & \mathrm{I}_{3\times3} \\ 0_{3\times3} & 0_{3\times3} \end{bmatrix}, \quad \mathrm{G}(t) = \begin{bmatrix} 0_{3\times3} \\ \mathrm{I}_{3\times3} \end{bmatrix}, \text{ and} \tag{4}$$

$\boldsymbol{\beta}$ is an Brownian motion process of diffusion

$$\mathrm{Q_c} = \begin{bmatrix} \sigma^2_{\text{plane}}\mathrm{I}_{2\times2} & 0_{2\times1} \\ 0_{1\times2} & \sigma^2_{\text{altitude}} \end{bmatrix}, \tag{5}$$

where σ^2_{plane} represents the velocity errors on the East-North plane and $\sigma^2_{\text{altitude}}$ represents the velocity errors in the vertical direction. We can write the solution of equation (3) as a difference equation [13]

$$\begin{aligned} \mathbf{x}_k &= \Phi_{k-1}\mathbf{x}_{k-1} + \mathbf{w}_{k-1} \\ &\stackrel{\triangle}{=} \mathbf{f}_{k-1}(\mathbf{x}_{k-1}) + \mathbf{w}_{k-1} \end{aligned} \tag{6}$$

where $\mathbf{x}_k = \mathbf{x}(t_k)$,

$$\Phi_{k-1} = e^{(t_k - t_{k-1})\mathrm{F}} = \begin{bmatrix} \mathrm{I}_{3\times 3} & \Delta t_k \mathrm{I}_{3\times 3} \\ 0_{3\times 3} & \mathrm{I}_{3\times 3} \end{bmatrix}, \quad (7)$$

$\Delta t_k = t_k - t_{k-1}$, and $\mathbf{w}_{k-1}$ is white, zero mean and Gaussian noise, so that

$$\begin{aligned} \mathrm{Q}_{k-1} = \mathrm{V}(\mathbf{w}_{k-1}) &= \int_{t_{k-1}}^{t_k} \Phi(t_k, t)\mathrm{G}(t)\mathrm{Q}_\mathrm{c}\mathrm{G}(t)^T \Phi(t_k, t)^T dt \\ &= \begin{bmatrix} \frac{\Delta t_k^3}{3}\mathrm{Q}_\mathrm{c} & \frac{\Delta t_k^2}{2}\mathrm{Q}_\mathrm{c} \\ \frac{\Delta t_k^2}{2}\mathrm{Q}_\mathrm{c} & \Delta t_k \mathrm{Q}_\mathrm{c} \end{bmatrix}. \end{aligned} \quad (8)$$

2.3 Measurement equation

In this study, we use quite general measurement equations and we do not restrict ourselves on any specific satellite system (e.g. GPS, GALILEO) or mobile phone network (e.g. GSM, 3G).

2.3.1 Satellite measurements

From satellites we get usually two different measurements: pseudorange (PR) and delta pseudorange (DPR) measurements [8]. We denote ρ_i^s the pseudorange measurement from the ith satellite and $\dot{\rho}_i^\mathrm{s}$ the delta pseudorange measurement from the ith satellite. The measurement equations are

$$\rho_i^\mathrm{s} = \|\mathbf{r}_i^\mathrm{s} - \mathbf{r}_\mathrm{u}\| + b + \epsilon_{\rho_i^\mathrm{s}}, \quad (9)$$

$$\begin{aligned} \dot{\rho}_i^\mathrm{s} &= \frac{(\mathbf{r}_i^\mathrm{s} - \mathbf{r}_\mathrm{u})^T}{\|\mathbf{r}_i^\mathrm{s} - \mathbf{r}_\mathrm{u}\|}(\mathbf{v}_i^\mathrm{s} - \mathbf{v}_\mathrm{u}) + \dot{b} + \epsilon_{\dot{\rho}_i^\mathrm{s}} \\ &\triangleq (\mathbf{u}_i^\mathrm{s})^T(\mathbf{v}_i^\mathrm{s} - \mathbf{v}_\mathrm{u}) + \dot{b} + \epsilon_{\dot{\rho}_i^\mathrm{s}}, \end{aligned} \quad (10)$$

where $\mathbf{r}_i^\mathrm{s}$ is the ith satellite position vector, $\mathbf{v}_i^\mathrm{s}$ is the ith satellite velocity vector, b is clock bias in meters, $\dot{b}$ is clock drift, $\mathbf{u}_i^\mathrm{s}$ is the unit vector from the user to the ith satellite, $\epsilon_{\rho_i^\mathrm{s}}$ is PR error term and $\epsilon_{\dot{\rho}_i^\mathrm{s}}$ is DPR error term. Let n_s be the number of satellites, then the measurement equations are

$$\boldsymbol{\rho}^\mathrm{s} = \begin{bmatrix} \|\mathbf{r}_1^\mathrm{s} - \mathbf{r}_\mathrm{u}\| \\ \vdots \\ \|\mathbf{r}_{n_\mathrm{s}}^\mathrm{s} - \mathbf{r}_\mathrm{u}\| \end{bmatrix} + b\mathbf{1} + \boldsymbol{\epsilon}_\rho^\mathrm{s} \triangleq \mathbf{h}_\rho^\mathrm{s}(\mathbf{r}_\mathrm{u}) + b\mathbf{1} + \boldsymbol{\epsilon}_\rho^\mathrm{s}, \quad (11)$$

$$\dot{\boldsymbol{\rho}}^\mathrm{s} = \mathrm{diag}(\mathrm{U}^\mathrm{s}(\mathrm{V}^\mathrm{s})^T) - \mathrm{U}^\mathrm{s}\mathbf{v}_\mathrm{u} + \dot{b}\mathbf{1} + \boldsymbol{\epsilon}_{\dot{\rho}}^\mathrm{s} \quad (12)$$

where

$$\begin{aligned} &\boldsymbol{\rho}^\mathrm{s} = [\rho_1^\mathrm{s}, \ldots, \rho_{n_\mathrm{s}}^\mathrm{s}]^T,\ \boldsymbol{\epsilon}_\rho^\mathrm{s} = [\epsilon_{\rho_1^\mathrm{s}}, \ldots, \epsilon_{\rho_{n_\mathrm{s}}^\mathrm{s}}]^T, \\ &\dot{\boldsymbol{\rho}}^\mathrm{s} = [\dot{\rho}_1^\mathrm{s}, \ldots, \dot{\rho}_{n_\mathrm{s}}^\mathrm{s}]^T,\ \boldsymbol{\epsilon}_{\dot{\rho}}^\mathrm{s} = [\epsilon_{\dot{\rho}_1^\mathrm{s}}, \ldots, \epsilon_{\dot{\rho}_{n_\mathrm{s}}^\mathrm{s}}]^T, \\ &\mathrm{U}^\mathrm{s} = [\mathbf{u}_1^\mathrm{s}, \ldots, \mathbf{u}_{n_\mathrm{s}}^\mathrm{s}]^T,\ \mathrm{V}^\mathrm{s} = [\mathbf{v}_1^\mathrm{s}, \ldots, \mathbf{v}_{n_\mathrm{s}}^\mathrm{s}]^T, \text{ and} \\ &\mathbf{1} \text{ is a vector of 1's.} \end{aligned} \quad (13)$$

We suppose that $n_s \geq 2$, otherwise we do not use satellite measurements. We get difference measurements when we multiply earlier equations by $\mathrm{D} \in \mathbb{R}^{(n_s-1)\times n_\mathrm{s}}$, where $\mathrm{D}\mathbf{1} = \mathbf{0}$ and $\mathrm{rank}(D) = n_\mathrm{s} - 1$. In simulations, we use $\mathrm{D} = \begin{bmatrix} \mathrm{I} & -\mathbf{1} \end{bmatrix}$. The difference measurement equations are

$$\mathrm{D}\boldsymbol{\rho}^\mathrm{s} = \mathrm{D}\mathbf{h}_\rho^\mathrm{s}(\mathbf{r}_\mathrm{u}) + b\mathrm{D}\mathbf{1} + \mathrm{D}\boldsymbol{\epsilon}_\rho^\mathrm{s} = \mathrm{D}\mathbf{h}_\rho^\mathrm{s}(\mathbf{r}_\mathrm{u}) + \mathrm{D}\boldsymbol{\epsilon}_\rho^\mathrm{s}, \quad (14)$$

$$\begin{aligned} \mathrm{D}\dot{\boldsymbol{\rho}}^\mathrm{s} &= \mathrm{D}(\mathrm{diag}(\mathrm{U}^\mathrm{s}(\mathrm{V}^\mathrm{s})^T) - \mathrm{U}^\mathrm{s}\mathbf{v}_\mathrm{u} + \dot{b}\mathbf{1} + \boldsymbol{\epsilon}_{\dot{\rho}}^\mathrm{s}) \\ &= \mathrm{D}(\mathrm{diag}(\mathrm{U}^\mathrm{s}(\mathrm{V}^\mathrm{s})^T) - \mathrm{U}^\mathrm{s}\mathbf{v}_\mathrm{u}) + \mathrm{D}\boldsymbol{\epsilon}_{\dot{\rho}}^\mathrm{s} \\ &\triangleq \mathrm{D}\mathbf{h}_{\dot{\rho}}^\mathrm{s}(\mathbf{r}_\mathrm{u}, \mathbf{v}_\mathrm{u}) + \mathrm{D}\boldsymbol{\epsilon}_{\dot{\rho}}^\mathrm{s}. \end{aligned} \quad (15)$$

2.3.2 Base station measurements

There are many possible different measurements in base station positioning, such as time of arrival (TOA), round trip delay (RTD), received signal strength (RSS), time difference of arrival (TDOA), angle of arrival (AOA), and cell identity (Cell-ID). [4, 18, 19, 20] We can also use cell average altitude for positioning if it is known. TOA, RTD and RSS have the same mathematical form

$$\rho_i^\mathrm{b} = \|\mathbf{r}_i^\mathrm{b} - \mathbf{r}_\mathrm{u}\| + \epsilon_{\rho_i^\mathrm{b}}, \quad (16)$$

where $\mathbf{r}_i^\mathrm{b}$ is ith base station position vector and $\epsilon_{\rho_i^\mathrm{b}}$ is error term. Let n_b be the number of base stations, then the measurement equations are

$$\boldsymbol{\rho}^\mathrm{b} = \begin{bmatrix} \|\mathbf{r}_1^\mathrm{b} - \mathbf{r}_\mathrm{u}\| \\ \vdots \\ \|\mathbf{r}_{n_\mathrm{b}}^\mathrm{b} - \mathbf{r}_\mathrm{u}\| \end{bmatrix} + \boldsymbol{\epsilon}_\rho^\mathrm{b} \triangleq \mathbf{h}_\rho^\mathrm{b}(\mathbf{r}_\mathrm{u}) + \boldsymbol{\epsilon}_\rho^\mathrm{b}, \quad (17)$$

where

$$\boldsymbol{\rho}^\mathrm{b} = [\rho_1^\mathrm{b}, \ldots, \rho_{n_\mathrm{b}}^\mathrm{b}]^T,\ \boldsymbol{\epsilon}_\rho^\mathrm{b} = [\epsilon_{\rho_1^\mathrm{b}}, \ldots, \epsilon_{\rho_{n_\mathrm{b}}^\mathrm{b}}]^T. \quad (18)$$

In this study, we do not use AOA or Cell-ID measurements.

2.3.3 Compound measurements

All measurements (11, 12, 18) can be written in a compound form

$$\mathbf{y}_k = \mathbf{h}_k(\mathbf{x}_k) + \mathbf{v}_k, \quad (19)$$

where

$$\mathbf{y}_k = \begin{bmatrix} \boldsymbol{\rho}_k^\mathrm{s} \\ \dot{\boldsymbol{\rho}}_k^\mathrm{s} \\ \boldsymbol{\rho}_k^\mathrm{b} \end{bmatrix} \text{ and } \mathbf{h}_k(\mathbf{x}_k) = \begin{bmatrix} \mathrm{D}\mathbf{h}_{k\rho}^\mathrm{s}(\mathbf{r}_{k\mathrm{u}}) \\ \mathrm{D}\mathbf{h}_{k\dot{\rho}}^\mathrm{s}(\mathbf{r}_{k\mathrm{u}}, \mathbf{v}_{k\mathrm{u}}) \\ \mathbf{h}_{k\rho}^\mathrm{b}(\mathbf{r}_{k\mathrm{u}}) \end{bmatrix}.$$

Measurement errors are

$$\mathbf{v}_k = \begin{bmatrix} \mathrm{D}\boldsymbol{\epsilon}_{k\rho}^\mathrm{s} \\ \mathrm{D}\boldsymbol{\epsilon}_{k\dot{\rho}}^\mathrm{s} \\ \boldsymbol{\epsilon}_{k\rho}^\mathrm{b} \end{bmatrix}, \text{ and } \mathrm{V}(\mathbf{v}_k) \triangleq \mathrm{R}_k.$$

2.4 Initial state

Filtering is performed within the framework of sequential Bayesian estimation, which requires the initial state $\mathbf{x}_0$. We assume that this initial state is Gaussian so

$$\mathbf{x}_0 \sim \mathrm{N}(x_0, \mathrm{P}_0). \quad (20)$$

One possibility to get the initial state is to use the first position and velocity solutions (see Section 3.3).

3 Filters

The Kalman filter extensions considered are Extended Kalman Filter (EKF), Second Order Extended Kalman Filter (EKF2) and Position Kalman Filter (PKF). The common feature of these filters and one reason why we call these filters Kalman filter extensions is that these filters "remember" and use only the last state mean and covariance matrices. These filters solve approximately the filtering problem (see Section 2).

Initial state	$\mathrm{E}(\mathbf{x}_0) = x_0, \mathrm{V}(\mathbf{x}_0) = \mathrm{P}_0$
State dynamic	$\mathbf{x}_{k+1} = \mathbf{f}_k(\mathbf{x}_k) + \mathbf{w}_k$
	$\mathrm{E}(\mathbf{w}_k) = \mathbf{0}, \mathrm{V}(\mathbf{w}_k) = \mathrm{Q}_k$
Measurement equation	$\mathbf{y}_k = \mathbf{h}_k(\mathbf{x}_k) + \mathbf{v}_k$
	$\mathrm{E}(\mathbf{v}_k) = \mathbf{0}, \mathrm{V}(\mathbf{v}_k) = \mathrm{R}_k$

3.1 EKF

The Extended Kalman Filter solves the filtering problem by linearizing the measurement function. EKF is very commonly used in satellite-based positioning and it has also been applied in hybrid positioning [12]. The EKF algorithm is [1, 7]

Algorithm 1 (EKF).

Prior mean	$\hat{x}_k^- = \mathbf{f}_{k-1}(\hat{x}_{k-1})$
Prior covariance	$\hat{\mathrm{P}}_k^- = \Phi_{k-1}\hat{\mathrm{P}}_{k-1}\Phi_{k-1}^T + \mathrm{Q}_{k-1}$
	$\Phi_{k-1} = \frac{\partial \mathbf{f}_{k-1}(\mathbf{x}_{k-1})}{\partial \mathbf{x}_{k-1}}\Big\vert_{\mathbf{x}_{k-1}=\hat{x}_{k-1}}$
Posterior mean	$\hat{x}_k = \hat{x}_k^- + \mathrm{K}_k(y_k - \mathbf{h}_k(\hat{x}_k^-))$
Posterior covariance	$\hat{\mathrm{P}}_k = (\mathrm{I} - \mathrm{K}_k\mathrm{H}_k)\hat{\mathrm{P}}_k^-$
	$\mathrm{H}_k = \frac{\partial \mathbf{h}_k(\mathbf{x}_k)}{\partial \mathbf{x}_k}\Big\vert_{\mathbf{x}_k=\hat{x}_k^-}$
Kalman gain	$\mathrm{K}_k = \hat{\mathrm{P}}_k^-\mathrm{H}_k^T(\mathrm{H}_k\hat{\mathrm{P}}_k^-\mathrm{H}_k^T + \mathrm{R}_k)^{-1}$

In hybrid positioning, the derivative of $\mathbf{h}_k(\mathbf{x}_k)$ (19) is

$$\mathrm{H}_k = \begin{bmatrix} \mathrm{D} & 0 & 0 \\ 0 & \mathrm{D} & 0 \\ 0 & 0 & \mathrm{I}_{n_\mathrm{b}\times n_\mathrm{b}} \end{bmatrix} \begin{bmatrix} -\mathrm{U}^\mathrm{s} & 0_{n_\mathrm{s}\times 3} \\ \dot{\mathrm{U}}^\mathrm{s}_{\mathrm{V}^\mathrm{s}} - \dot{\mathrm{U}}^\mathrm{s}_{\mathbf{v}_\mathrm{u}} & -\mathrm{U}^\mathrm{s} \\ -\mathrm{U}^\mathrm{b} & 0_{n_\mathrm{b}\times 3} \end{bmatrix}, \tag{21}$$

where $\mathrm{U}^\mathrm{s} = [\mathbf{u}_1^\mathrm{s}, \ldots, \mathbf{u}_{n_\mathrm{s}}^\mathrm{s}]^T$, $\mathbf{u}_i^\mathrm{s} = \frac{\mathbf{r}_i^\mathrm{s} - \mathbf{r}_\mathrm{u}}{\|\mathbf{r}_i^\mathrm{s} - \mathbf{r}_\mathrm{u}\|}$, $\mathrm{U}^\mathrm{b} = [\mathbf{u}_1^\mathrm{b}, \ldots, \mathbf{u}_{n_\mathrm{b}}^\mathrm{b}]^T$, $\mathbf{u}_i^\mathrm{b} = \frac{\mathbf{r}_i^\mathrm{b} - \mathbf{r}_\mathrm{u}}{\|\mathbf{r}_i^\mathrm{b} - \mathbf{r}_\mathrm{u}\|}$,

$$\dot{\mathrm{U}}^\mathrm{s}_{\mathbf{v}_\mathrm{u}} = \begin{bmatrix} -\mathbf{v}_\mathrm{u}^T\mathrm{H}^e_{\|\mathbf{r}_1^\mathrm{s} - \mathbf{r}_\mathrm{u}\|} \\ \vdots \\ -\mathbf{v}_\mathrm{u}^T\mathrm{H}^e_{\|\mathbf{r}_{n_\mathrm{s}}^\mathrm{s} - \mathbf{r}_\mathrm{u}\|} \end{bmatrix}$$

and

$$\dot{\mathrm{U}}^\mathrm{s}_{\mathrm{V}^\mathrm{s}} = \begin{bmatrix} -(\mathbf{v}_1^\mathrm{s})^T\mathrm{H}^e_{\|\mathbf{r}_1^\mathrm{s} - \mathbf{r}_\mathrm{u}\|} \\ \vdots \\ -(\mathbf{v}_{n_\mathrm{s}}^\mathrm{s})^T\mathrm{H}^e_{\|\mathbf{r}_{n_\mathrm{s}}^\mathrm{s} - \mathbf{r}_\mathrm{u}\|} \end{bmatrix},$$

where Hessian matrix of $\|\mathbf{r}_i^\mathrm{s} - \mathbf{r}_\mathrm{u}\|$ is

$$\mathrm{H}^e_{\|\mathbf{r}_i^\mathrm{s} - \mathbf{r}_\mathrm{u}\|} = \frac{1}{\|\mathbf{r}_i^\mathrm{s} - \mathbf{r}_\mathrm{u}\|}\left(\mathrm{I} - \frac{(\mathbf{r}_i^\mathrm{s} - \mathbf{r}_\mathrm{u})}{\|\mathbf{r}_i^\mathrm{s} - \mathbf{r}_\mathrm{u}\|}\frac{(\mathbf{r}_i^\mathrm{s} - \mathbf{r}_\mathrm{u})^T}{\|\mathbf{r}_i^\mathrm{s} - \mathbf{r}_\mathrm{u}\|}\right).$$

3.2 EKF2

The Second Order Extended Kalman Filter is an elaboration of EKF that takes into consideration the nonlinearity of the measurement models. Modified Gaussian Second Order Filter [7, 14] is the same as EKF2. The EKF2 algorithm is [1]

Algorithm 2 (EKF2).

$$\begin{aligned}
&\hat{x}_{k+1}^- = \mathbf{f}_k(\hat{x}_k) + \tfrac{1}{2}\textstyle\sum_{i=1}^{n_x}\mathbf{e}_i\,\mathrm{tr}(\Phi_k^{e_i}\hat{\mathrm{P}}_k)\\
&\quad \Phi_k^{e_l} = \left(\frac{\partial^2(\mathbf{f}_k(\mathbf{x}_k))_l}{\partial x_j \partial x_i}\right)\Big|_{\mathbf{x}_k=\hat{x}_k}\\
&\hat{\mathrm{P}}_k^- = \Phi_{k-1}\hat{\mathrm{P}}_{k-1}\Phi_{k-1}^T + \mathrm{Q}_{k-1} + \mathrm{Q}_{extra}\\
&\quad \mathrm{Q}_{extra} = \tfrac{1}{2}\textstyle\sum_{i=1}^{n_x}\sum_{j=1}^{n_x}\mathbf{e}_i\mathbf{e}_j^T\,\mathrm{tr}(\Phi_k^{e_i}\hat{\mathrm{P}}_k\Phi_k^{e_j}\hat{\mathrm{P}}_k)\\
&\quad \Phi_{k-1} = \frac{\partial \mathbf{f}_{k-1}(\mathbf{x}_{k-1})}{\partial \mathbf{x}_{k-1}}\Big|_{\mathbf{x}_{k-1}=\hat{x}_{k-1}}\\
&\hat{y}_k^- = \mathbf{h}_k(\hat{x}_k^-) + \tfrac{1}{2}\textstyle\sum_{i=1}^{n_y}\mathbf{e}_i\,\mathrm{tr}(\mathrm{H}_k^{e_i}\hat{\mathrm{P}}_k^-)\\
&\quad \mathrm{H}_k^{e_l} = \left(\frac{\partial^2(\mathbf{h}_k(\mathbf{x}_k))_l}{\partial x_j \partial x_i}\right)\Big|_{\mathbf{x}_k=\hat{x}_k^-}\\
&\hat{x}_k = \hat{x}_k^- + \mathrm{K}_k(y_k - \hat{y}_k^-)\\
&\hat{\mathrm{P}}_k = (\mathrm{I} - \mathrm{K}_k\mathrm{H}_k)\hat{\mathrm{P}}_k^-\\
&\quad \mathrm{H}_k = \frac{\partial \mathbf{h}_k(\mathbf{x}_k)}{\partial \mathbf{x}_k}\Big|_{\mathbf{x}_k=\hat{x}_k^-}\\
&\quad \mathrm{K}_k = \hat{\mathrm{P}}_k^-\mathrm{H}_k^T(\mathrm{H}_k\hat{\mathrm{P}}_k^-\mathrm{H}_k^T + \mathrm{R}_k + \mathrm{R}_{extra})^{-1}\\
&\quad \mathrm{R}_{extra} = \tfrac{1}{2}\textstyle\sum_{i=1}^{n_y}\sum_{j=1}^{n_y}\mathbf{e}_i\mathbf{e}_j^T\,\mathrm{tr}(\mathrm{H}_k^{e_i}\hat{\mathrm{P}}_k^-\mathrm{H}_k^{e_j}\hat{\mathrm{P}}_k^-)
\end{aligned}$$

where n_x is the dimension of state, in our applications $n_x = 6$, n_y is the number of measurements, which can be a function of time. In hybrid positioning the Hessian matrix of $\mathbf{e}_l^T\mathbf{h}_k(\mathbf{x}_k)$ (19) is

$$\begin{aligned}
\mathrm{H}_k^{e_l} &= \sum_{j=1}^{n_\mathrm{s}}\begin{bmatrix} (D)_{lj}\mathrm{H}^e_{\|\mathbf{r}_j^\mathrm{s} - \mathbf{r}_\mathrm{u}\|} & 0 \\ 0 & 0 \end{bmatrix}, \text{ if } l = 1, \ldots, n_\mathrm{s},\\
\mathrm{H}_k^{e_l} &= \sum_{j=1}^{n_\mathrm{s}}(D)_{lj}\begin{bmatrix} \frac{\partial}{\partial \mathbf{r}_\mathrm{u}}\left(\mathrm{H}^e_{\|\mathbf{r}_j^\mathrm{s} - \mathbf{r}_\mathrm{u}\|}(\mathbf{v}_\mathrm{u} - \mathbf{v}_j^\mathrm{s})\right) & \mathrm{H}^e_{\|\mathbf{r}_j^\mathrm{s} - \mathbf{r}_\mathrm{u}\|} \\ \mathrm{H}^e_{\|\mathbf{r}_j^\mathrm{s} - \mathbf{r}_\mathrm{u}\|} & 0 \end{bmatrix},\\
&\quad \text{if } l = n_\mathrm{s} + 1, \ldots, 2n_\mathrm{s},\\
\mathrm{H}_k^{e_l} &= \begin{bmatrix} \mathrm{H}^e_{\|\mathbf{r}_l^\mathrm{b} - \mathbf{r}_\mathrm{u}\|} & 0 \\ 0 & 0 \end{bmatrix}, \text{ if } l = 2n_\mathrm{s} + 1, \ldots, 2n_\mathrm{s} + n_\mathrm{b},
\end{aligned} \tag{22}$$

where

$$\frac{\partial}{\partial \mathbf{r}_\mathrm{u}}\left(\mathrm{H}^e_{\|\mathbf{r}_j^\mathrm{s} - \mathbf{r}_\mathrm{u}\|}(\mathbf{v}_\mathrm{u} - \mathbf{v}_j^\mathrm{s})\right) = \frac{(\mathrm{I} - \mathbf{u}_j^\mathrm{s}\mathbf{u}_j^{\mathrm{s}T})(\mathbf{v}_\mathrm{u} - \mathbf{v}_j^\mathrm{s})^T\mathbf{u}_j^\mathrm{s}}{\|\mathbf{r}_j^\mathrm{s} - \mathbf{r}_\mathrm{u}\|^2} + \frac{(\mathbf{v}_\mathrm{u} - \mathbf{v}_j^\mathrm{s})\mathbf{u}_j^{\mathrm{s}T} + \mathbf{u}_j^\mathrm{s}(\mathbf{v}_\mathrm{u} - \mathbf{v}_j^\mathrm{s})^T(\mathrm{I} - 2\mathbf{u}_j^\mathrm{s}\mathbf{u}_j^{\mathrm{s}T})}{\|\mathbf{r}_j^\mathrm{s} - \mathbf{r}_\mathrm{u}\|^2}.$$

3.3 PKF

The Position Kalman Filter works by filtering a sequence of static position and velocity solutions. The idea is that we first solve position and velocity and then filter these; this idea is called two-stage estimator [3]. When we have enough measurements, we can find position and velocity for example by Weighted Least Squares (WLS) or closed-form methods [17]. WLS also approximates the errors of solution. At times instants when there are not enough measurements to fix position and velocity, we do not use any measurements. The PKF algorithm is

Algorithm 3 (PKF). *First solve static position and velocity and then use Kalman filter.*

Prior mean	$\hat{x}_k^- = \mathbf{f}_{k-1}(\hat{x}_{k-1})$
Prior cov.	$\hat{\mathrm{P}}_k^- = \Phi_{k-1}\hat{\mathrm{P}}_{k-1}\Phi_{k-1}^T + \mathrm{Q}_{k-1}$
	$\Phi_{k-1} = \frac{\partial \mathbf{f}_{k-1}(\mathbf{x}_{k-1})}{\partial \mathbf{x}_{k-1}}\Big\vert_{\mathbf{x}_{k-1}=\hat{x}_{k-1}}$
Posterior mean	$\hat{x}_k = \hat{x}_k^- + \mathrm{K}_k(y_k - \mathrm{H}_k\hat{x}_k^-)$
	$\mathrm{H}_k = \begin{cases} \mathrm{I}_{6\times 6}, & pos.\,and\,vel. \\ \left[\begin{array}{cc} \mathrm{I}_{3\times 3} & 0_{3\times 3}\end{array}\right], & only\,pos. \end{cases}$
Posterior cov.	$\hat{\mathrm{P}}_k = (\mathrm{I} - \mathrm{K}_k\mathrm{H}_k)\hat{\mathrm{P}}_k^-$
Kalman gain	$\mathrm{K}_k = \hat{\mathrm{P}}_k^-\mathrm{H}_k^T(\mathrm{H}_k\hat{\mathrm{P}}_k^-\mathrm{H}_k^T + \mathrm{R}_k)^{-1}$

Because now $\mathbf{f}_{k-1}(\hat{x}_{k-1}) = \Phi_{k-1}\hat{x}_{k-1}$ the previous algorithm is Kalman filter algorithm [7], but it is important to notice that errors of position solutions are not independent from state dynamics errors, so the system does not fulfill the assumptions of Kalman Filter.

3.4 Nonlinearities

Our model has nonlinearities only in the measurement model. We say that the measurement nonlinearities are significant if they are comparable to, or larger than, the measurement noise [7]:

$$\mathrm{R}_{extra} \gtrsim \mathrm{R}. \tag{23}$$

In the following we use the notation $\mathrm{A} \geq \mathrm{B}$ to signify that $\mathrm{A} - \mathrm{B}$ is positive semidefinite.

First we study the significance of nonlinearities in satellite measurements, $i, j \in \{1, \ldots, 2 \cdot n_\mathrm{s}\}$:

$$\begin{aligned} \|\mathrm{R}_{extra}\| &\leq \frac{n_y}{2}\max_{i,j}|\mathrm{tr}(\mathrm{H}^{e_i}\hat{\mathrm{P}}^-\mathrm{H}^{e_j}\hat{\mathrm{P}}^-)| \\ &\leq \frac{n_y n_x}{2}\|\hat{\mathrm{P}}^-\|^2 \max_i \|\mathrm{H}^{e_i}\|^2 \end{aligned} \tag{24}$$

If we suppose that $n_y \leq 10$, $\mathrm{D} = \left[\begin{array}{cc} \mathrm{I} & -\mathbf{1}\end{array}\right]$, $\|\mathbf{v}_\mathrm{u}\| \leq 5\ 000(\frac{\mathrm{m}}{\mathrm{s}})$, $\|\hat{\mathrm{P}}^-\| \leq 100^2$, these last two approximations are quite overpessimistic in personal satellite positioning. We know that $\|\mathbf{r}_i^\mathrm{s} - \mathbf{r}_\mathrm{u}\| \geq 20\ 000$ (km), $\|\mathbf{v}_i^\mathrm{s}\| \leq 5\ 000(\frac{\mathrm{m}}{\mathrm{s}})$ [8]. Thus we get

$$\|\mathrm{R}_{extra}\| \leq \frac{n_y n_x}{2}\|\hat{\mathrm{P}}^-\|^2\frac{4n_x^2}{\|\mathbf{r}_i^\mathrm{s} - \mathbf{r}_\mathrm{u}\|^2} \leq 0.00108. \tag{25}$$

In our simulation, the smallest eigenvalue of R, when we consider satellite measurements, is 0.1^2. So $\mathrm{R}_{extra} < \mathrm{R}$ and there are no significant nonlinearities in satellite measurements. The difference between R_{extra} and R is even bigger if we use only satellite pseudorange measurements. Because of this, we linearize all satellites measurements and use those in our simulations.

Secondly, we concentrate on base station measurements nonlinearities, $i \in \{2 \cdot n_\mathrm{s} + 1, \ldots, 2 \cdot n_\mathrm{s} + n_\mathrm{b}\}$. Now we suppose that $\hat{\mathrm{P}}^- = \|\hat{\mathrm{P}}^-\|\mathrm{I}$.

$$\begin{aligned} \|\mathrm{R}_{extra}\| &\geq \frac{1}{2}|\mathrm{tr}(\mathrm{H}^{e_i}\hat{\mathrm{P}}^-\mathrm{H}^{e_i}\hat{\mathrm{P}}^-)| \\ &\geq \frac{\|\hat{\mathrm{P}}^-\|^2}{\|\mathbf{r}_i^\mathrm{b} - \mathbf{r}_\mathrm{u}\|^2} \end{aligned} \tag{26}$$

In our simulation the eigenvalues of R, when we consider base station measurements, are 80^2. It is very common in urban areas that the distance from base station is very short, say $\|\mathbf{r}_i^\mathrm{b} - \mathbf{r}_\mathrm{u}\| \approx 250$ m, but the error can be quite large, say $\|\hat{\mathrm{P}}^-\| \approx 150^2$. We get

$$\|\mathrm{R}_{extra}\| \gtrsim 90^2 > 80^2 = \|\mathrm{R}\|, \tag{27}$$

so there are in some cases significant nonlinearities in base station range measurements.

3.5 Inconsistency tests

We say that filter is consistent if inequality

$$\mathrm{E}_{f_{cpdf}(\mathbf{x}_k)}\left[(\mathbf{x}_k - \hat{\mathbf{x}}_k)(\mathbf{x}_k - \hat{\mathbf{x}}_k)^T\right] \leq \mathrm{P}_k \tag{28}$$

holds in every $k = 1, 2, \ldots$ [9]. The normalized estimation error squared test (NEES) and the normalized innovation squared test (NIS) [1] are popular ways of testing filter inconsistency [9, 10, 16]. Both NEES and NIS tests assume that distributions are Gaussian, so that test statistics are chi-square distributed. However we know that distributions are usually not Gaussian. Because of this we apply Chebyshev's inequality to our hypothesis testing. Our null hypothesis is

$$H_0 : \mathrm{E}_{f_{cpdf}(\mathbf{x}_k)}\left[(\mathbf{x}_k - \hat{\mathbf{x}}_k)(\mathbf{x}_k - \hat{\mathbf{x}}_k)^T\right] \leq \mathrm{P}_k \tag{29}$$

We assume that $\det(\mathrm{P}_k) \neq 0$. Now there is a matrix A_k such that $\mathrm{P}_k = \mathrm{A}_k^{-1}(\mathrm{A}_k^T)^{-1}$. Hypothesis test statistic is

$$\|\psi_k\| = \|\mathrm{A}_k(\mathbf{x}_k - \hat{\mathbf{x}}_k)\|. \tag{30}$$

If H_0 is true then

$$\begin{aligned} n = \mathrm{tr}(\mathrm{A}_k\mathrm{P}_k\mathrm{A}_k^T) &\geq \mathrm{E}_{f_{cpdf}(\mathbf{x}_k)}\left[\mathrm{tr}(\psi_k\psi_k^T)\right] \\ &= \mathrm{E}_{f_{cpdf}(\mathbf{x}_k)}\left[\|\psi_k\|^2\right] \\ &\geq \int_{\|\psi_k\|\geq\epsilon} \|\psi_k\|^2 f_{cpdf}(\mathbf{x}_k)d\mathbf{x}_k \\ &\geq \epsilon^2\mathrm{P}(\|\psi_k\| \geq \epsilon) \\ \Rightarrow \mathrm{P}(\|\psi_k\| \geq \epsilon) &\leq \frac{n}{\epsilon^2}, \end{aligned} \tag{31}$$

where n is the dimension of $\mathbf{x}_k$. If α is the risk level then

$$\mathrm{P}\left(\|\psi_k\| \geq \sqrt{\frac{n}{\alpha}}\right) \leq \alpha. \tag{32}$$

So if $\|\psi_k\| \geq \sqrt{\frac{n}{\alpha}}$ is true, it indicates that the null hypothesis can be rejected at the risk level of α. We call this test *the general inconsistency test*. If we also assume that $\mathbf{x}_k - \hat{\mathbf{x}}_k$ is zero mean and Gaussian then $\|\psi_k\|^2 \sim \chi^2(n)$. This is the above-mentioned NEES. If we do not assume that $\det(\mathrm{P}_k) \neq 0$ we get (the same way as earlier (31))

$$\mathrm{P}\left(\|\mathbf{x}_k - \hat{\mathbf{x}}_k\| \geq \sqrt{\frac{\mathrm{tr}(\mathrm{P}_k)}{\alpha}}\right) \leq \alpha. \tag{33}$$

4 Simulations

In our simulations, we use East-North-Up (ENU) coordinate system. We assume that errors $\epsilon_{\rho_i^s}$, $\epsilon_{\dot{\rho}_i^s}$ and $\epsilon_{\rho_i^b}$ are zero mean, independent Gaussian white noise, with

$$\sigma_{\rho^s} = 10 \text{ m}, \sigma_{\dot{\rho}^s} = 0.1 \frac{\text{m}}{\text{s}} \text{ and } \sigma_{\rho^b} = 80 \text{ m}. \quad (34)$$

As parameters of state dynamics we use

$$\sigma^2_{\text{plane}} = 2 \frac{\text{m}^2}{\text{s}^3}, \sigma^2_{\text{altitude}} = 1 \frac{\text{m}^2}{\text{s}^3}. \quad (35)$$

The first parameter is the same as in [12]. The initial state $\mathbf{x}_0$ of our simulations is

$$\mathbf{x}_0 \sim \text{N}(x_0, \text{P}_0), \quad (36)$$

where $x_0 = [\mathbf{r}_0^T, \mathbf{0}^T]^T$, $\mathbf{r}_0$ is true place at time t_0 and

$$\text{P}_0 = \begin{bmatrix} 100^2 \text{I}_{3\times3} & 0_{3\times3} \\ 0_{3\times3} & 10^2 \text{I}_{3\times3} \end{bmatrix}. \quad (37)$$

The positions and velocities of satellites are based on real ephemeris data. Ephemeris data was measured in the Tampere University of Technology campus region on June 18th 2003. Base station positions are $\mathbf{r}_1^b = [1\,000, 0, 0]$, $\mathbf{r}_2^b = [-1\,000, 0, 0]$ and $\mathbf{r}_3^b = [0, 1\,000, 0]$, see Figure 1. Measurements and true route are simulated using measurements equation (19) and state dynamics (6) with given parameters. In some tests we simulate also altitude measurements. The altitude measurements are modelled as same kind of measurements as base station range measurements, with the "base station" in the center of Earth.

A typical simulation is shown Figure 1, which shows base stations, true route (red, 2 minutes), filters mean: PKF (black), EKF (blue), EKF2 (magenta), and covariance ellipses which illustrate dispersion of distribution. The covariance ellipses satisfy the equation

$$(\mathbf{x} - \hat{x})^T \hat{\text{P}}^{-1} (\mathbf{x} - \hat{x}) = 2.2173. \quad (38)$$

The constant was chosen so that if the distribution is Gaussian then there is 67% probability mass inside the ellipse. Ellipses are drawn every half minute. In this example, we get three base stations range measurements and altitude information every second.

From Figure 1, we can see that filters work very similarly in this case and that they give much better position estimates than the static WLS solutions. Table 1 shows that in many cases all filters work very similarly.

We generated one hundred true routes and for every true route 10×18 measurement sets so that every satellite (SV) and base station (BS) set have ten measurement sets for every true route. The satellites and base stations are the same throughout all simulations, although we would get better results if we used different satellites and base stations in different time instants. Tables 1 and 2 have error limits from these simulations. Filters' error limits are in Table 1 and WLS error limits are in Table 2, where we also have a column which tells how many times WLS does not have a unique position solution. In these tables the 67% column gives limit so that 67% of all 2 dimensional errors (norm of true position minus posterior mean) are smaller than this limit, and similarly for the 95% column. Every measurement set has also altitude measurement, except the measurement sets where BS column has $\emptyset$ sign.

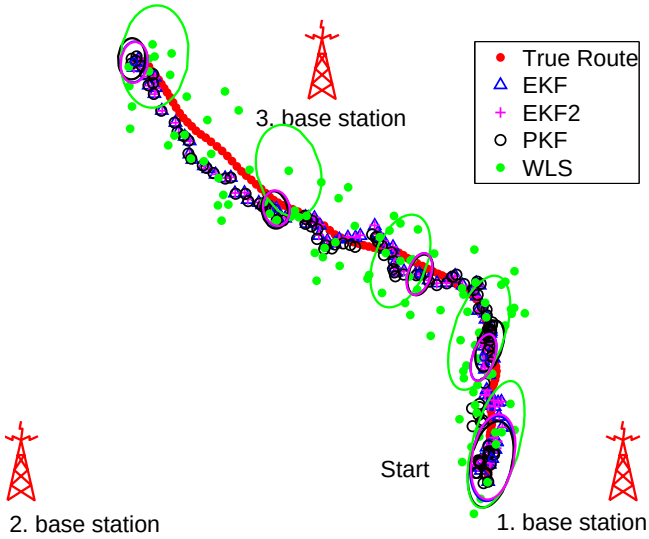

Figure 1: Simulation example with measurements from three base station and altitude information.

Table 1: Two-dimensional error limits for filters, in simulations have 100 true routes and every true route was run 10 times

Meas.		PKF		EKF		EKF2	
SV	BS	67%	95%	67%	95%	67%	95%
0	1	944	2448	731	2731	764	2160
0	2	944	2448	212	2243	403	2038
0	3	61	117	56	104	56	104
2	$\emptyset$	944	2448	710	2119	710	2119
2	0	944	2448	698	2117	698	2117
2	1	944	2448	59	219	60	214
2	2	37	74	35	72	35	72
2	3	35	70	33	69	33	69
3	$\emptyset$	944	2448	247	710	247	710
3	0	18	31	14	26	14	26
3	1	18	30	13	25	13	25
3	2	17	29	12	24	12	24
3	3	17	29	12	23	12	23
4	$\emptyset$	5	9	5	9	5	9
4	0	5	9	5	9	5	9
4	1	4	8	4	8	4	8
4	2	4	9	4	9	4	9
4	3	4	8	4	8	4	8

In Table 1 we see that EKF and EKF2 errors have noticeable difference only when we have only one or two base station range measurements. If we consider 95% errors limits we see that EKF2 gives better position estimates than EKF. Actually, when we have only one base station range measurement, PKF gives better estimate than EKF although PKF has no position solutions (see Table 2). We see in Section 4.2 that in this case EKF is very often inconsistent. It is useful to notice that the ratio of 95% error limits and 67% error limits is usually about two.

There are however some cases, especially (0,2) and (2,1), (SV,BS) combinations, where this ratio is much bigger. We see that in all of these cases where this ratio is about three or bigger there is a problem with consistency (see Section 4.2). PKF has noticeable difference with respect to EKF or EKF2 only when there are no unique position solutions. We can also see that even quite rough altitude information gives much better position estimates than without that information.

Table 2: Two dimensional error limits for WLS and how many times we do not have unique WLS solution.

Meas.		WLS		no unique WLS
SV	BS	67%	95%	solution (%)
0	1	∞	∞	100
0	2	∞	∞	100
0	3	150	∞	7
2	$\emptyset$	∞	∞	100
2	0	∞	∞	100
2	1	∞	∞	100
2	2	85	190	1
2	3	81	187	2
3	$\emptyset$	∞	∞	100
3	0	39	68	0
3	1	36	65	1
3	2	35	62	1
3	3	33	61	2
4	$\emptyset$	20	36	0
4	0	20	36	0
4	1	20	36	0
4	2	20	36	0
4	3	20	35	0

In Table 2, we see that WLS position solutions' (estimated) errors are many times larger than estimated errors of filters, so it is reasonable to use statistical approach (filters) with as many measurements as possible if we want more accurate position estimates.

4.1 Requirements of CGALIES and FCC

Both American federal Communications Commission (FCC) and European Coordination Group on Access to Location Information for Emergency Services (CGALIES) have their own requirements emergency call positioning accuracy. These requirements are briefly summarized in Tables 3 and 4.

The limits in Table 3 are intended for 67% of calls, but in the future the requirements may be tightened to apply to 95% of calls. A summary of CGALIES 67% accuracy requirements is approximately 150 m in urban environment and 500 m in rural environment [11]. The main difference between urban and rural environments is that in urban environment there is a high density of mobile phone base stations but the satellite visibility is reduced. Vice versa, in rural environment there is good satellite visibility but the mobile phone base stations are very sparsely laid out [6].

If we compare CGALIES and FCC requirements and our simulation results, we can conclude that WLS estimates

Table 3: CGALIES requirements for location (values indicated between parenthesis correspond to the requirements obtained through a questionnaire to the Member States)[11]

CGALIES	Urban	Rural
Caller cannot provide any information	10 - 150 m (10 - 50 m)	10 - 500 m (10 - 100 m)
Caller can provide general information	25 - 150 m (10 - 50 m)	50 - 500 m (30 - 100 m)

Table 4: FCC requirements for location[5]

FCC	Accuracy for 67% of calls	Accuracy for 95% of calls
Handset-based	50 m	150 m
Network-based	100 m	300 m

satisfy all requirements only if they use at least three satellite measurements and altitude information. WLS estimates satisfy CGALIES and FCC network-based requirements if they use measurements from two satellites, altitude information and at least two base stations. WLS satisfy CGALIES requirements by a whisker with altitude information and measurements from three base stations.

With the above-mentioned measurement sets, all three filters satisfy almost all requirements. Only the FCC handset-based requirement of accuracy for 67% of calls is not fulfilled with altitude information and measurements from three base stations. EKF and EKF2 satisfy also CGALIES and FCC network-based requirements with altitude information and measurements from two satellites and one base station. Furthermore, EKF and EKF2 satisfy CGALIES rural environment requirement with measurements from three satellites or two base stations and altitude information. Although in our simulation, using measurements from only one base station does not satisfy any requirements, it is possible that in urban environments with very high base station density these requirements can be satisfied. This is possible if base stations are always sufficiently close to users. Of course, then the base station where measurements come from must be changed quite often.

4.2 Consistency

In our simulations, we saw that there are consistency problems with some base station and satellite measurement combinations. Now we study whether the filters work correctly or not. One way to test this is to use the general inconsistency test, which tells if true estimate errors coincide with the error covariance matrix given by the filter (see Section 3.5).

Figure 2 shows one case where EKF estimate veers away from the true route and gets stuck in an incorrect solution branch. In this case, filters get measurements from two base stations and altitude information for the first 110 seconds. During the last 10 seconds, there is an additional base station measurement, making unique WLS position fixes possible.

The covariance ellipses as defined in (38) are drawn at time instants t_0, t_{60}, t_{110}, t_{111}, and t_{120}. We see that here EKF covariance matrices are very small if we compare them to true estimates errors. Because of this, EKF is inconsistent which is also verified by the general inconsistency test (see Figure 3). Note that in this kind of situation NIS test is not relevant, for example in this case EKF passes NIS test when it uses measurements only from two base station and altitude information. From Figure 2, we can also see that after the third base station becomes available at t_{110}, it takes a long time for EKF to become consistent again.

In this example, the covariance matrices of EKF2 are large enough so that EKF2 is not inconsistent (see Figure 3). Also, although the PKF estimate remains at the starting point for the first 110 seconds, the filter is not inconsistent as its covariance grows fast enough.

It is useful to notice that both EKF2 and PKF start giving accurate estimates as soon as the third base station becomes available. Note that although both filters EKF2 and PKF are not inconsistent in this case, we can say that EKF2 gives better, or more accurate, estimates.

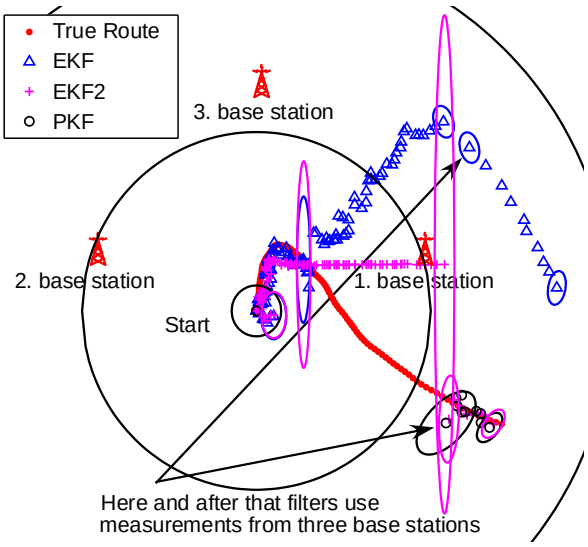

Figure 2: EKF estimate veers away from the true route and gets stuck in an incorrect solution branch. EKF2 increases covariance matrix.

All in all, we can observe from the foregoing example that it is very important that a filter be consistent. Now we study more precisely how often and with which measurement combinations filters are inconsistent. We use the same simulations as in Table 1. All general inconsistency test results which are non-zero are tabulated in Table 5. Tabulated quantity tells how many percent of 1 000 runs have at least one time instant in which the filter is inconsistent at some risk level. We use both 5% and 1% risk level.

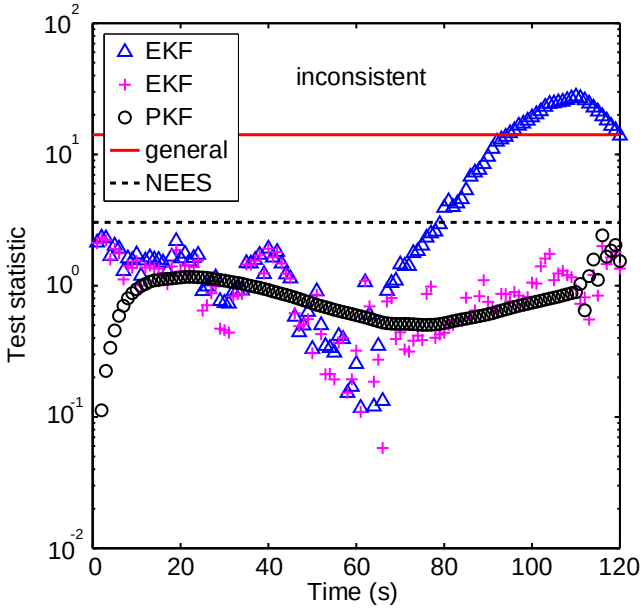

Figure 3: Inconsistency test of the situation of Figure 2. In this case, only EKF fails this test, test statistic is bigger than red line. Black dashed line is NEES test. Risk level of both test is $\alpha = 0.01$.

Table 5: Percentage of times filters are inconsistent (the general inconsistency test), same simulations than Table 1.

Meas.			EKF		EKF2	
SV	BS	α	5%	1%	5%	1%
0	1		71	50	14	9
0	2		40	32	15	15
2	$\emptyset$		6	0	6	0
2	0		6	0	6	0
2	1		6	5	5	4
3	$\emptyset$		4	0	4	0

First of all, PKF never has problems with consistency and because of this PKF is not mentioned in Table 5. From Tables 5 and 2 we can see that EKF and EKF2 only have problems with consistency when the system is underdetermined (when there is no unique position solution). These problems are significant when there are base station measurements. EKF2 works better than EKF. However, EKF2 does have some problems with consistency. One reason is that although EKF2 takes into consideration the nonlinearity of the base station range measurement models, there are still small errors. These small errors can accumulate because the measurement model depends on the previous state estimate. EKF also has this same problem that measurement model depends on the previous state estimate. PKF does not have this problem and this is one reason why PKF never fails this test.

5 Conclusions

In this article, we have shown that nonlinearities are insignificant in satellite measurements, but often significant in base station measurements. In these cases EKF2 works better than EKF, and the 95% error limits of EKF2 are smaller and EKF2 is not so often inconsistent. Unfortunately, EKF2 also is sometimes inconsistent. PKF does not have a problem with consistency, but the error limit of PKF is usually larger than in other filters. Our simulations results indicate that static WLS position estimates can fulfill FCC and CGALIES requirements only when there are satellite measurements available. On the other hand, filtered position estimates can fulfill these requirements even using only base station measurements.

References

[1] Bar-Shalom, Yaakov; Li, Rong X. & Kirubarajan, Thiagalingam 2001. *Estimation with Applications to Tracking and Navigation, Theory Algorithms and Software* John Wiley & Sons. 558 s.

[2] Brown, Robert Grover 1983. *Introduction to Random Signal Analysis and Kalman Filtering.* John Wiley & Sons. 347 s.

[3] Chaffee, James W. & Abel, Jonathan S. 1992. *The GPS Filtering Problem.* IEEE Position Location and Navigation Symposium, Monterey, CA, 1992.

[4] Drane, Christopher; Macnaughtan, Malcolm & Scott, Craig 1998. *Positioning GSM Telephones.* IEEE Communications Magazine, April 1998, pages 46-59.

[5] Federal Communication Commission website: http://www.fcc.gov

[6] Heinrichs, Günter; Dovis, Fabio; Gianola, Manuela & Mulassano, Paolo 2004. *Navigation and Communication Hybrid Positioning with a Common Receiver Architecture.* Proceedings of The European Navigation Conference GNSS 2004.

[7] Jazwinski, Andrew H. 1970. *Stochastic Processes and Filtering Theory.* Mathematics in Science and Engineering, Vol. 64. Academic Press. 378 p.

[8] Kaplan, Elliot D. (ed.) 1996. *Understanding GPS: Principles and Applications.* Norwood, Artech House. 629 s.

[9] Lefebvre, Tine; Bruyninckx, Herman & De Schutter, Joris 2004. *Kalman Filters for Non-linear Systems: a Comparison of Performance.* International Journal of Control, Vol. 77, No. 7, May 2004.

[10] Lerro, Don & Bar-Shalom, Yaakov 1993. *Tracking With Debiased Consistent Converted Measurements Versus EKF.* IEEE Transactions on Aerospace and Electronic Systems, Vol. 29, No. 3, July 1993.

[11] Ludden, Brendan et al., *Report on Implementation Issues Related to Access to Location Information by Emergency Services (E112) in the European Union.* C.G.A.L.I.E.S. Final Report, Feb. 2002.

[12] Ma, Changlin 2003. *Integration of GPS and Cellular Networks to Improve Wireless Location Performance.* ION GPS/GNSS 2003 proceedings, pages 1585-1596.

[13] Maybeck, Peter S. 1979. *Stochastic Models, Estimation, and Control, Vol. 1.* Mathematics in Science and Engineering, Vol. 141. Academic Press. 432 s.

[14] Maybeck, Peter S. 1982. *Stochastic Models, Estimation, and Control, Vol. 2.* Mathematics in Science and Engineering, Vol. 141-2. Academic Press. 289 p.

[15] Ristic, Branko; Arulampalam, Sanjeev & Gordon, Neil 2004. *Beyond the Kalman Filter, Particle Filters for Tracking Applications.* Boston, London, Artech House. 299 s.

[16] Schlosser, M. S. & Kroschel, K. 2004. *Limits in tracking with extended Kalman filters.* IEEE Transactions on Aerospace and Electronic Systems, Vol. 40, No. 4, Oct. 2004.

[17] Sirola, Niilo; Piché, Robert & Syrjärinne, Jari 2003. *Closed-Form Solutions for Hybrid Cellular/GPS Positioning.* Proceedings of ION GPS/GNSS 2003, pages 1613-1619.

[18] Spirito, Maurizio A.; Pöykkö, Sami & Knuuttila, Olli 2001. *Experimental Performance of Methods to Estimate the Location of Legacy Handsets in GSM.* IEEE Vehicular Technology Conference, 2001, pages 2716-2720.

[19] Syrjärinne Jari 2001. *Studies of modern techniques for personal positioning.* Tampere, Tampere University of Technology, Publications 319. 180 p.

[20] Vossiek, Martin; Wiebking, Leif; Gulden, Peter; Wieghardt, Jan; Hoffmann, Clemens & Heide, Patric 2003. *Wireless Local Positioning.* IEEE microwave magazine, Dec. 2003, pages 77-86.